

## Experimental Probing of Quantum-Well Eigenstates

Jean-Yves Marzin and Jean-Michel Gérard

Laboratoire de Bagneux, Centre National d'Etudes des Telecommunications, 92220 Bagneux, France

(Received 29 November 1988)

We measured the spatial variation of the probability densities in the first few electron states of a GaAs/Al<sub>x</sub>Ga<sub>1-x</sub>As quantum well. This result was obtained from the optical determination of the energies of the bound states as a function of the position of a highly localized perturbation, consisting of one isoelectronic substituted cation plane containing either indium (attractive potential) or aluminum (repulsive potential). A series of samples was prepared, each with the probe plane in a different position, scanning thus the whole width of the quantum wells.

PACS numbers: 73.60.Br, 03.65.-w, 71.50.+t, 78.55.Cr

Probing local structural or electronic properties of solids remains an experimental challenge. One powerful approach is to incorporate and test built-in localized probes, such as isoelectronic (or deep-level) substituted impurities, which create a short-range potential. In particular, the optical study of the GaAs<sub>x</sub>P<sub>1-x</sub> semiconductors doped with N or Cu yielded an insight into the local arrangement of atoms around the impurity and thus into the alloy disorder in these materials.<sup>1,2</sup> Au planes were also used to probe the penetration depth of a surface state in Ag(111),<sup>3</sup> and deep-level impurities to predict the band lineups in semiconductor heterojunctions.<sup>4-6</sup>

In this Letter, we extend for the first time this approach to the use of a planar isoelectronic perturbation to measure the spatial dependence of the probability density associated with a discrete set of eigenstates. We establish the validity of this technique in the case of a GaAs-Al<sub>x</sub>Ga<sub>1-x</sub>As semiconductor quantum well, for the first bound electron levels. Despite the fact that it may be used in a large number of multilayered structures, this method is indeed well suited for semiconductor quantum wells in which the electron and hole densities (averaged over a constituent bulk material unit cell) are spatially modulated along one direction (the growth axis  $z$ ). Finally, with molecular-beam epitaxy, samples containing very thin layers (such as short-period<sup>7</sup> superlattices and "delta-doped" heterostructures<sup>8</sup>) can be grown. In our experiment, this high degree of control allowed the insertion of one-monolayer-thick planar probes in the studied structure, during its growth process. Two substituting species, yielding either a repulsive or an attractive potential, have been successfully used in two independent series of experiments.

The electronic properties of quantum wells are well described by effective-mass models. In this framework, the eigenstates in a quantum well structure correspond to wave functions  $\Psi_i^n(x, y, z)$  given by

$$\Psi_{i,k_x,k_y}^n(x, y, z) = F_i^n(z) e^{ik_x x} e^{ik_y y} u_0^n(x, y, z). \quad (1)$$

$u_0^n$ , assumed to be identical in the two constitutive bulk materials, is the zone-center Bloch eigenfunction for the band  $n$  (conduction or valence).  $F_i^n(z)$  is the envelope

function for the  $i$ th bound state corresponding to band  $n$  and is an eigenfunction of the one-dimensional Hamiltonian

$$H_0 = P_z^2/2m^* + V^n(z), \quad (2)$$

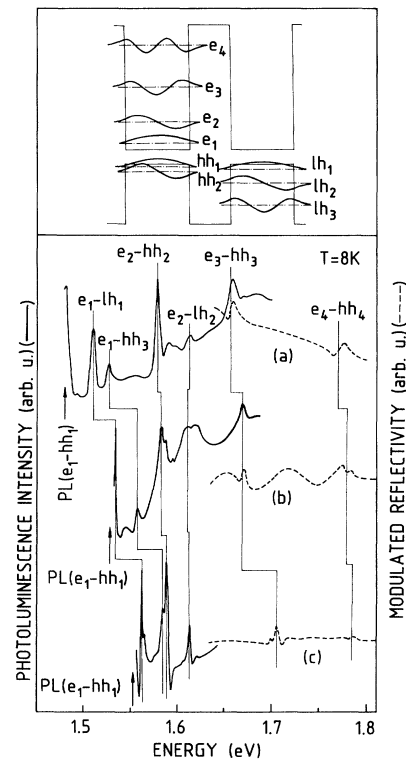


FIG. 1. Typical photoluminescence excitation (full line) and modulated reflectivity (dashed line) spectra obtained for (a) the indium plane at the center of the well (series A); (b) the reference sample; and (c) the aluminum plane at the center of the well (series B). For more clarity, the modulated spectra have been indicated only in the high-energy range. The  $e_1$ - $lh_1$  transition energy is obtained either from the photoluminescence energy or modulated reflectivity. Inset: Schematic of the expected envelope wave functions for the first electron and hole levels.

where  $V^n(z)$  is a square potential describing the  $z$  dependence of the  $n$ th band edge in the structure. The eigenstates of (2) are labeled  $e_i$ ,  $hh_i$ , and  $lh_i$  (of energies  $E_i^e$ ,  $E_i^{hh}$ , and  $E_i^{lh}$ ), respectively, for electron, heavy-hole, and light-hole bands. The expected envelope wave functions for the first confined levels are shown schematically in the inset of Fig. 1.  $|F_i^n(z_0)|^2$  is a slowly varying function on the scale  $a_z$  of the bulk lattice parameter, hereafter referred to as the probability density envelope (PDE), and is the probability density averaged over a slab of width  $a_z$  around  $z = z_0$ . Approximate values for the PDE's can be obtained, as will be discussed later, if a localized perturbation is inserted in the structure and its position varied from sample to sample. For the GaAs/AlGaAs quantum wells we studied, the perturbation consisted of the isoelectronic substitution of a (100) cation plane, either by In (attractive potential) or by Al (repulsive potential).

The samples were grown by molecular-beam epitaxy on GaAs(100) substrates. They consist of multi-quantum-well structures with six GaAs wells, each 160 Å wide, separated by 85-Å  $\text{Al}_{0.29}\text{Ga}_{0.71}\text{As}$  barriers. In a first series (A) of samples, one indium monolayer was inserted in each period and its location varied from sample to sample. In eight samples, we probe the first grown half of the (symmetric) GaAs well. In one additional sample, the In plane is located in its second half. The last sample was a reference sample without In. In a second series (B) of samples, aluminum was inserted instead of indium, and six samples (including a reference one) were fabricated.

The low-temperature (10 K) optical transition energies were determined both from photoluminescence exci-

tation spectroscopy (where the emission intensity at a given wavelength is recorded as a function of the scanned excitation wavelength) and from wavelength-modulated reflectivity. Figure 1 shows typical spectra displayed here for the reference sample and the samples with the isoelectronic plane situated at the center of the well for series A and B. The transitions observed for the reference sample are assigned to  $e_i$ - $hh_j$  and  $e_i$ - $lh_j$  from their energies calculated with a simple effective-mass-type model.<sup>9</sup> The nature of the transitions for the "perturbed" samples can be deduced by continuity from sample to sample without ambiguity.

Figure 2 shows the energies of these various transitions as functions of the position  $z_0$  of the electronic plane for the two series of samples. The energy variations (tens of meV) are large compared with the experimental errors (1 meV). They are, as expected, of opposite sign in series A and B and qualitatively reflect the shapes of the PDE's in the unperturbed quantum well. Assuming a perturbation  $W^e \delta(z - z_0)$  for the electrons and  $W^{hh(lh)} \delta(z - z_0)$  for the heavy (light) holes, the first-order  $z_0$  dependence of the  $e_i$ - $hh_i$  ( $-lh_i$ ) transition energy is given by

$$\Delta E^{z_0}(e_i\text{-}hh_i \text{ (-}lh_i)) = W^e |F_i^e(z_0)|^2 + W^{hh(lh)} |F_i^{hh(lh)}(z_0)|^2. \quad (3)$$

Since the unperturbed envelope wave functions are not very different for  $e_i$  and  $hh_i$ , the transition energies roughly map the corresponding PDE in both  $e_i$  and  $hh_i$  levels across the structure (in particular, the number and location of nodes for different values of  $i$ ). Nevertheless, this first-order description is not sufficient to extract quantitatively the PDE's, because the localized potential mixes different quantum-well states.

To go further, consider the one-dimensional Hamiltonian  $H_0$  of Eq. (2), having a series of eigenfunctions  $F_i(z)$  with discrete energies  $E_i$ , and a localized perturbation  $W \delta(z - z_0)$ . The eigenenergies  $E_i^{z_0}$  of the perturbed Hamiltonian  $H_1 = H_0 + W \delta(z - z_0)$  either keep the unperturbed value  $E_i$  if  $F_i(z_0) = 0$  (i.e., if the probe plane is located at a node of the PDE), or satisfy the (infinite) set of equations

$$\sum_{E_j \neq E_i^{z_0}} \frac{|F_j(z_0)|^2}{E_i^{z_0} - E_j} = \frac{1}{W}. \quad (4)$$

In principle, the PDE's,  $|F_j(z_0)|^2$ , can be extracted from the  $E_j$  and  $E_i^{z_0}$  values using (4).

A finite set ( $j \leq p$ ), corresponding to the lowest energy levels, is accessible experimentally so that only approximate values  $\rho_j(z_0)$  for the PDE's can be obtained. The first  $p$  equations of system (4) are considered under the form

$$\sum_{E_j \neq E_i^{z_0}}^{j=p} \frac{|F_j(z_0)|^2}{E_i^{z_0} - E_j} = \frac{1}{W} - \sum_{\substack{m=p+1 \\ E_m \neq E_i^{z_0}}}^{\infty} \frac{|F_m(z_0)|^2}{E_i^{z_0} - E_m} = \frac{1}{W_i}. \quad (5)$$

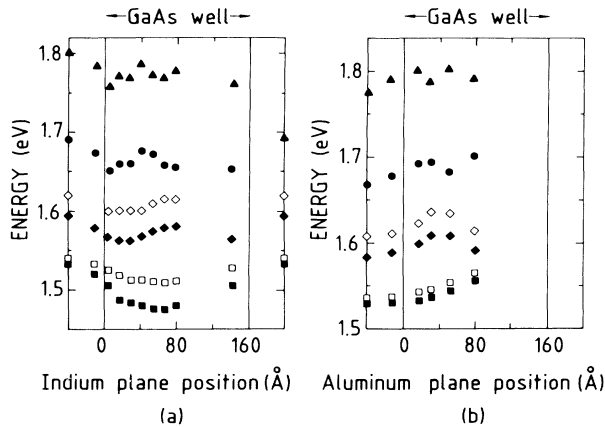


FIG. 2. Experimental transition energies obtained at 10 K, as functions of the position of the isoelectronic plane, (a) for series A (In plane) and (b) for series B (Al plane).  $\blacksquare$ ,  $e_1$ - $hh_1$ ;  $\square$ ,  $e_1$ - $lh_1$ ;  $\blacklozenge$ ,  $e_2$ - $hh_2$ ;  $\diamond$ ,  $e_2$ - $lh_2$ ;  $\bullet$ ,  $e_3$ - $hh_3$ ; and  $\blacktriangle$ ,  $e_4$ - $hh_4$ . The transitions energies plotted at  $-40$  and  $200$  Å (far in barrier) are those of the reference samples. While they are also observed (Fig. 1), transitions  $e_1$ - $hh_3$  are not indicated.

The right-hand sides of Eqs. (5),  $1/W_i$ , depend *a priori* on  $z_0$  and  $i$ , and include the correction to the perturbation potential due to the remote levels. The simplest approximation is to take them as independent of  $z_0$ . The corresponding errors on the  $\rho_j$ 's will be discussed later in the specific case of a quantum well.

If all the  $E_j^{z_0}$  are different from the  $E_j$ 's, the inversion of system (5) yields directly  $\rho_i$ , for  $i$  varying from 1 to  $p$ , as a function of the  $W_i$ 's. This procedure is repeated at a series of  $z_0$ . The normalization conditions (in our specific case on one period of the superlattice) for the  $\rho_i$ 's can be approximated by discrete sums over the sampled values:

$$\sum_{z_0=z_a}^{z_0=z_b} \rho_i(z) \Delta z = 1. \quad (6)$$

The  $p$  conditions (6) allow elimination of the  $W_i$ 's. The above procedure can be used regardless of the sign and strength of the potential  $W$ .

Experimentally, the resolution of this method is limited by several factors: the finite spatial extension of the perturbing potential, the spacing between the sampled  $z_0$  (here 10 Å), and finally the energy range where the levels are determined. The latter point leads to a cutoff frequency, *a priori* unknown and system dependent. It limits the resolution to about  $d/N\pi$  for a quantum well when the  $N$  first levels are considered (15 Å in our case).

To proceed to the quantitative analysis of our experimental data, it is necessary to extract the energy differences, which appear in Eq. (5), from the transition energies:

$$E(e_i\text{-hh}_j) = E_g + E_i^e + E_j^{\text{hh}} - E^{\text{ex}}(e_i, \text{hh}_j), \quad (7)$$

where  $E_g$  is the GaAs band gap, and  $E^{\text{ex}}(e_i, \text{hh}_j)$  is the  $e_i\text{-hh}_j$  exciton binding energy. We make two further assumptions for that last step. First, we assume that the energies  $E_1^{\text{hh}}$  and  $E_2^{\text{hh}}$  are the same in all structures, and equal to those in the reference sample. This is reasonable since the valence-band discontinuities between InAs (or AlAs) and GaAs are smaller than the conduction-band ones ( $W^{\text{hh}}$  and  $W^{\text{lh}}$  smaller than  $W^e$ ), and the

effective masses for the light holes are rather low. This assumption is more accurate in the case of InAs since light holes are only slightly bound by an InAs monolayer inserted in a GaAs matrix.<sup>10</sup> The second assumption is to take as binding energies for all  $e_i\text{-hh}_i$  (respectively,  $e_i\text{-lh}_i$ ) excitons, and for all samples, those obtained experimentally in Ref. 11, for a sample similar to the reference sample; i.e.,  $E^{\text{ex}} = 6.5$  meV (9 meV). For  $e_i\text{-hh}_j$  excitons, with  $i \neq j$ , we take the binding energies equal to zero.  $E_i^e$  and  $E_i^{\text{hh}}$  can then be deduced from the observed transitions ( $e_i\text{-hh}_i$ ,  $e_i\text{-lh}_i$ , for  $1 \leq i \leq 3$ , and  $e_i\text{-hh}_3$ ). We took the symmetry of the quantum well into account in the normalizing conditions (6).

The results are not very sensitive to the values of  $E_1^{\text{hh}}$  and  $E_2^{\text{hh}}$ . If they are assumed to be the same in all samples, they only enter the calculation via the energy difference  $E_2^{\text{hh}} - E_1^{\text{hh}}$ . This quantity can be obtained experimentally in the most asymmetric samples where an additional  $e_2\text{-lh}_1$  transition is observed. Our analysis then does not rely on a particular model to extract the electron energy levels, but on the correct assignment of the observed transitions.

Figure 3 shows the PDE's for the first three electron levels deduced from the experimental data independently for the two series of samples, together with the calculated effective-mass values. The indicated error bars include the errors on the determination of the transition energies, exciton binding energies, and light-hole confinement energies and are indicated up to 3 standard deviations. The increasing error bars for  $\rho_1$ ,  $\rho_2$ , and  $\rho_3$  are due to a decreasing experimental precision for  $E_1^e$ ,  $E_2^e$ , and  $E_3^e$ . It should be noted that the uncertainty in the sample parameters (which is difficult to estimate) was not taken into account in these error bars. The overall agreement is very good for both series, confirming that both types of perturbations can be used.

While, in principle, the heavy-hole wave functions can be determined from the same set of data, the precision for the  $\rho$ 's is much poorer in this case because of the smaller energy variations of the heavy-hole levels due to the perturbation.

Finally, the  $z_0$  dependence of the  $1/W_i$  of Eq. (4) can

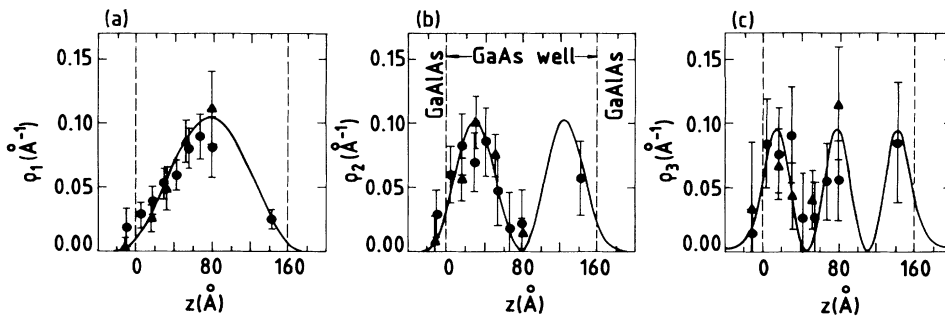


FIG. 3. Experimental PDE's  $\rho$  for (a)  $e_1$ , (b)  $e_2$ , and (c)  $e_3$ , compared to the theoretical effective-mass result. Dots and triangles indicate experimental results obtained on series A and B, respectively.

be estimated for the case of a quantum well with infinite barriers. This provides an upper limit on their fluctuations around a mean value, resulting in an error for the  $\rho_i$ 's which is much smaller than our experimental error.

The oscillator strengths of the transitions are also dependent on the location of the isoelectronic plane: Isoelectronic doping is one way to efficiently break the symmetry of the quantum wells, as confirmed by the observation of certain parity-forbidden transitions only in the most asymmetric samples. The exploitation of these features, and the discussion of additional information that can be obtained from our data, e.g., strength of the perturbative potential, are out of the scope of this Letter, and will appear elsewhere.

Beyond yielding satisfying results in this simple case, our technique can be useful in layered systems where there may be a doubt in the spatial probability distribution in a given electronic state. This can occur in semiconductor superlattices which can be of "type 2,"<sup>12</sup> the first electron states being then mostly confined in one material and the hole states in the other. The introduction of an isoelectronic probe in one or the other of the two constituents and optical studies of the perturbed and unperturbed structures should prove unambiguously the occurrence of this situation.

The authors are grateful to D. Paquet, M. Bensoussan, I. Abram, and K. Elcess for their advice and comments,

and to J. Primot for the x-ray characterization of the samples. Laboratoire de Bagnex is Unité Associée No. 250 du Centre National de la Recherche Scientifique.

<sup>1</sup>H. Mariette, J. Chevallier, and P. Leroux-Hugon, *Phys. Rev. B* **21**, 5706 (1980).

<sup>2</sup>L. Samuelson, S. Nilsson, Z. G. Wang, and H. G. Grimmeiss, *Phys. Rev. Lett.* **53**, 1501 (1984).

<sup>3</sup>T. C. Hsieh, T. Miller, and T. C. Chiang, *Phys. Rev. Lett.* **55**, 2483 (1985).

<sup>4</sup>M. J. Caldas, A. Fazzio, and A. Zunger, *Appl. Phys. Lett.* **45**, 671 (1984).

<sup>5</sup>J. M. Langer and H. Heinrich, *Phys. Rev. Lett.* **55**, 1414 (1985).

<sup>6</sup>C. Delerue, M. Lannoo, and J. M. Langer, *Phys. Rev. Lett.* **61**, 199 (1988).

<sup>7</sup>A. C. Gossard, P. M. Petroff, W. Weigmann, R. Dingle, and A. Savage, *Appl. Phys. Lett.* **29**, 323 (1976).

<sup>8</sup>For example, K. Ploog, M. Hauser, and A. Fisher, *Appl. Phys. A* **45**, 233 (1988).

<sup>9</sup>G. Bastard, *Phys. Rev. B* **24**, 5693 (1981).

<sup>10</sup>J. M. Gerard and J. Y. Marzin, *Appl. Phys. Lett.* **53**, 568 (1988).

<sup>11</sup>R. T. Collins, L. Vina, W. I. Chang, L. Esaki, K. v. Klitzing, and K. Ploog, *Phys. Rev. B* **36**, 1531 (1987).

<sup>12</sup>For example, L. Esaki, in *Narrow Gap Semiconductors. Physics and Applications*, edited by W. Zawadzki, Lecture Notes in Physics Vol. 133 (Springer-Verlag, Berlin, 1980).